

A Semisynthetic Metalloenzyme Based on a Protein Cavity That Catalyzes the Enantioselective Hydrolysis of Ester and Amide Substrates

Ronald R. Davies and Mark D. Distefano*

Contribution from the Department of Chemistry, University of Minnesota, Minneapolis, Minnesota 55455

Received March 13, 1997[®]

Abstract: In an effort to prepare selective and efficient catalysts for ester and amide hydrolysis, we are designing systems that position a coordinated metal ion within a defined protein cavity. Here, the preparation of a protein-1,10-phenanthroline conjugate and the hydrolytic chemistry catalyzed by this construct are described. Iodoacetamido-1,10-phenanthroline was used to modify a unique cysteine residue in ALBP (adipocyte lipid binding protein) to produce the conjugate ALBP-Phen. The resulting material was characterized by electrospray mass spectrometry, UV/vis and fluorescence spectroscopy, gel filtration chromatography, and thiol titration. The stability of ALBP-Phen was evaluated by guanidine hydrochloride denaturation experiments, and the ability of the conjugate to bind Cu(II) was demonstrated by fluorescence spectroscopy. ALBP-Phen-Cu(II) catalyzes the enantioselective hydrolysis of several unactivated amino acid esters under mild conditions (pH 6.1, 25 °C) at rates 32–280-fold above the background rate in buffered aqueous solution. In 24 h incubations 0.70 to 7.6 turnovers were observed with enantiomeric excesses ranging from 31% *ee* to 86% *ee*. ALBP-Phen-Cu(II) also promotes the hydrolysis of an aryl amide substrate under more vigorous conditions (pH 6.1, 37 °C) at a rate 1.6×10^4 -fold above the background rate. The kinetics of this amide hydrolysis reaction fit the Michaelis–Menten relationship characteristic of enzymatic processes. The rate enhancements for ester and amide hydrolysis reported here are 10^2 – 10^3 lower than those observed for free Cu(II) but comparable to those previously reported for Cu(II) complexes.

Introduction

Enzymes perform chemical reactions with high specificity and rate enhancement in aqueous media at low temperatures and neutral pH. These features have made these catalysts attractive for a variety of purposes in medicine and industry. However, the use of naturally occurring enzymes is restricted by their inherent specificity. To circumvent this limitation, the development of artificial enzymes has received considerable attention. One approach for the design of new enzymes is to modify a known protein or enzyme at a defined site with a cofactor or new functional group to create a semisynthetic system with novel properties.^{1–10} A number of such constructs have been prepared resulting in a new generation of “enzyme-like” catalysts.¹¹ However, since most of these systems take

advantage of a substrate binding site present in the starting enzyme, their specificities are often limited to structures that bind to the native enzyme. This is a significant impediment for the development of catalysts with new specificities.

Our design for the development of new catalysts is based on the use of a protein cavity that can accommodate a variety of substrates.¹² By introducing catalytic functionality into the constrained environment of the cavity it should be possible to impart selectivity to chemical reactions occurring within. Different specificities and reactivities could then be optimized by mutagenesis of particular cavity residues. A key requirement for constructing this type of system is the availability of a suitable protein cavity. In this regard, adipocyte lipid binding protein (ALBP) is an excellent candidate. ALBP is a small, 131 amino acid, protein that possesses a 600 Å³ cavity formed from two orthogonal planes of antiparallel β -sheet secondary structure.¹³ This large cavity size provides ample space for both catalyst and putative substrate and effectively sequesters them from the exterior. Several crystal structures of ALBP with different ligands bound within the cavity have been solved as well as a number of additional structures of closely related fatty acid binding proteins.¹⁴ Recently, a structure of a similar protein complexed with palmitate was determined using NMR methods.¹⁵ All of these tertiary structures are quite similar despite their highly divergent primary sequences. This is important

[®] Abstract published in *Advance ACS Abstracts*, November 1, 1997.

(1) Collins, A. N.; Sheldrake, G. N.; Crosby, J. *Chirality in Industry: The Commercial Manufacture and Applications of Optically Active Compounds*; Collins, A. N., Sheldrake, G. N., Crosby, J., Eds.; John Wiley & Sons: Chichester, 1992.

(2) (a) Kaiser, E. T.; Lawrence, D. S. *Science* **1984**, *226*, 505–511. (b) Levine, H. L.; Nakagawa, Y.; Kaiser, E. T. *Biochem. Biophys. Res. Comm.* **1977**, *76*, 64–70.

(3) Corey, D. R.; Schultz, P. G. *Science* **1987**, *238*, 1401–1403.

(4) (a) Polgar, L.; Bender, M. L. *J. Am. Chem. Soc.* **1966**, *88*, 3153–3154. (b) Neet, K. E.; Koshland, D. E. *Proc. Natl. Acad. Sci. U.S.A.* **1966**, *56*, 1606–1609.

(5) Wu, Z. P.; Hilvert, D. *J. Amer. Chem. Soc.* **1989**, *111*, 4513–4514.

(6) Planas, A.; Kirsch, J. F. *Biochemistry* **1991**, *30*, 8268–8273.

(7) Wuttke, D. S.; Gray, H. B.; Fisher, S. L.; Imperiali, B. *J. Am. Chem. Soc.* **1993**, *115*, 8455–8456.

(8) Imperiali, B.; Roy, R. S. *J. Am. Chem. Soc.* **1994**, *116*, 12083–12084.

(9) Suckling, C. J.; Zhu, L. M. *Bioorg. Med. Chem. Lett.* **1993**, *3*, 531–534.

(10) Germanas, J. P.; Kaiser, E. T. *Biopolymers* **1990**, *29*, 39–43.

(11) (a) Bell, I. M.; Hilvert, D. *New Biocatalysts via Chemical Modification*; Bell, I. M., Hilvert, D., Eds.; John Wiley & Sons, Ltd.: Chichester, 1994; pp 73–88. (b) Schultz, P. G. *Science* **1988**, *240*, 426–433.

(12) Kuang, H.; Brown, M. L.; Davies, R. R.; Young, E. C.; Distefano, M. D. *J. Am. Chem. Soc.* **1996**, *118*, 10702–10706.

(13) Banaszak, L.; Winter, N.; Xu, Z.; Bernlohr, D. A.; Cowan, S.; Jones, T. A. *Adv. Protein Chem.* **1994**, *45*, 89–151.

(14) (a) Sacchettini, J. C.; Meininger, T. A.; Lowe, J. B.; Gordon, J. L.; Banaszak, L. J. *J. Biol. Chem.* **1987**, *262*, 5428–5430. (b) Sacchettini, J. C.; Gordon, J. L.; Banaszak, L. J. *J. Mol. Biol.* **1989**, *208*, 327–339. (c) Xu, Z.; Bernlohr, D. A.; Banaszak, L. J. *Biochemistry* **1992**, *31*, 3484–3492. (d) LaLonde, J. M.; Bernlohr, D. A.; Banaszak, L. J. *Biochemistry* **1994**, *33*, 4885–4895.

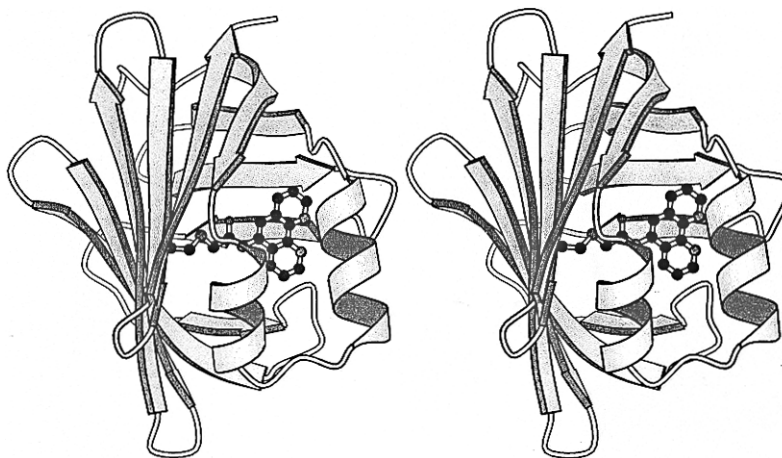


Figure 1. Stereoview of model of ALBP-Phen.

because it suggests that most of the cavity residues are amenable to substitution. Indeed, a number of mutagenesis studies have been carried out with ALBP and related fatty acid binding proteins resulting in very little change in the overall structure.¹⁶

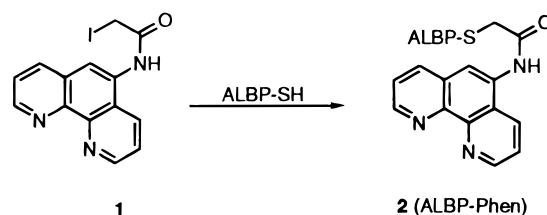
Transition metal complexes catalyze a diverse array of chemical reactions. The ligand system 1,10-phenanthroline has been attached to a number of proteins to perform oxidative chemistry.¹⁷ Cupric ions, Cu(II)-phenanthroline, and related metal-ligand systems have also been shown to promote the hydrolysis of esters and amides resulting in rate enhancements 10^5 – 10^6 -fold above the background rate.^{18–20} Based on these precedents, we decided to investigate the hydrolytic chemistry catalyzed by copper phenanthroline within the ALBP cavity.²¹

In the work described here, we have attached a phenanthroline ligand to a unique cysteine residue present in the interior of ALBP in order to position a Cu(II) ion within the protein cavity. The resulting semisynthetic metalloprotein, ALBP-Phen-Cu(II)

catalyzes the enantioselective hydrolysis of several *unactivated* amino acid esters; these include methyl, ethyl, and isopropyl esters of the amino acids alanine, tyrosine, and serine. Enantioselectivities as high as 86% *ee* and catalysis with as many as 7.6 turnovers in 24 h have been obtained. The hydrolysis of an aryl amide substrate and an aryl ester are also described.

Results

Preparation of ALBP-Phen. ALBP-Phen (**2**) was prepared by reacting iodoacetamido 1,10-phenanthroline (**1**) with ALBP at ambient temperature for 48 h as shown below. The extent of reaction with Cys₁₁₇ was quantitated by thiol titration with Ellman's reagent under denaturing conditions. Using this



method, alkylation efficiencies of 85–95% were typically obtained. A model for ALBP-Phen, based on the X-ray crystal structure of an oleic acid–ALBP complex, is shown in Figure 1.²²

Characterization of ALBP-Phen. Following preparation, ALBP-Phen was purified by gel filtration chromatography to remove unincorporated **1**, and the resulting protein was characterized by a number of spectroscopic and physical methods summarized in Table 1. Figure 2 shows the UV/vis spectra of ALBP (A) and ALBP-Phen (B) at equal concentrations. These spectra show that attachment of the phenanthroline moiety to

(15) Hodsdon, M. E.; Ponder, J. W.; Cistola, D. P. *J. Mol. Biol.* **1996**, *264*, 585–602.

(16) (a) Sha, R. S. C. D. K.; Xu, Z.; Banaszak, L. J.; Bernlohr, D. A. *J. Biol. Chem.* **1993**, *268*, 7885–7892. (b) Jiang, N.; Frieden, C. *Biochemistry* **1993**, *32*, 11015–11021. (c) Frieden, C.; Jiang, N.; Cistola, D. P. *Biochemistry* **1995**, *34*, 2724–2730. (d) Kim, K.; Cistola, D. P.; Frieden, C. *Biochemistry* **1996**, *35*, 7553–7558. (e) Cistola, D. P.; Kim, K.; Rogl, H.; Frieden, C. *Biochemistry* **1996**, *35*, 7559–7565. (f) Stump, D. G.; Chytil, F. *J. Biol. Chem.* **1991**, *266*, 4622–4630.

(17) (a) Sigman, D. S.; Chen, C.-H. B.; Gorin, M. B. *Nature* **1993**, *363*, 474–475. (b) Pan, C. Q.; Feng, J. A.; Finkel, S. E.; Landgraf, R.; Sigman, D.; Johnson, R. C. *Proc. Natl. Acad. Sci. U.S.A.* **1994**, *91*, 1721–1725. (c) Ebright, R. H.; Ebright, Y. W.; Pendergrast, P. S.; Gunasekera, A. *Proc. Natl. Acad. Sci. U.S.A.* **1990**, *87*, 2882–2886. (d) Francois, J. C.; Behmoaras, T. S.; Chassignol, M.; Thuong, N. T.; Sun, J. S.; Helene, C. *Biochemistry* **1988**, *27*, 2272–2276. (e) Sigman, D. S. *Acc. Chem. Res.* **1986**, *19*, 180–186. (f) Sigman, D. S.; Bruce, T. W.; Mazumder, A.; Sutton, C. L. *Acc. Chem. Res.* **1993**, *26*, 98–104.

(18) (a) Kroll, H. *J. Am. Chem. Soc.* **1952**, *74*, 2036–2039. (b) Bender, M. L.; Turnquist, B. W. *J. Amer. Chem. Soc.* **1957**, *79*, 1889–1893. (c) Meriwether, L.; Westheimer, F. H. *J. Am. Chem. Soc.* **1956**, *78*, 5119–5123.

(19) (a) Sayre, L. M.; Reddy, K. V.; Jacobson, A. R.; Tang, W. *Inorg. Chem.* **1992**, *31*, 935–937. (b) Reddy, K. V.; Jacobson, A. R.; Kung, J. I.; Sayre, L. M. *Inorg. Chem.* **1991**, *30*, 3520–3525. (c) Weijnen, J. G. J.; Koudijs, A.; Engbersen, J. F. J. *J. Chem. Soc., Perkin Trans. 2* **1991**, 1121–1125. (d) Weijnen, J. G. J.; Koudijs, A.; Engbersen, J. F. J. *Org. Chem.* **1992**, *57*, 7258–7265. (e) Nakon, R.; Rechani, P. R.; Angelici, R. J. *J. Am. Chem. Soc.* **1974**, *96*, 2117–2120.

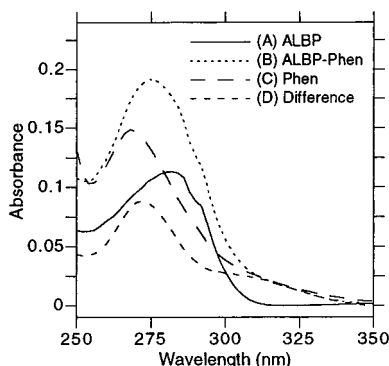
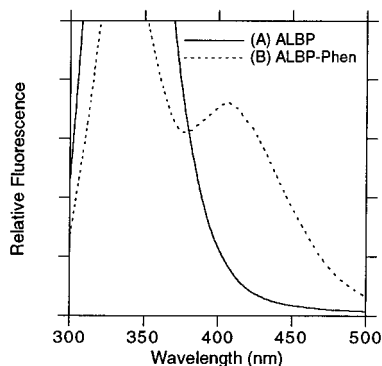
(20) (a) Brown, R. S.; Zamkane, M.; Cocho, J. L. *J. Am. Chem. Soc.* **1984**, *106*, 5222–5228. (b) Schepartz, A. R. B. *J. Am. Chem. Soc.* **1987**, *109*, 1814–1826. (c) Hay, R. W.; Basak, A. K. *Chem. Soc., Dalton Trans.* **1982**, 1819–1823. (d) Hay, R. W.; Banerjee, P. K. *J. Chem. Soc., Dalton Trans.* **1980**, 362–365. (e) Hay, R. W.; Banerjee, P. K. *J. Inorg. Biochem.* **1981**, *14*, 147–154. (f) Burgeson, I. E.; Kostic, N. M. *Inorg. Chem.* **1991**, *30*, 4299–4301. (g) Linkletter, B.; Chin, J. *Angew. Chem., Int. Ed. Engl.* **1995**, *34*, 472–474. (h) Buckingham, D. A.; Foster, D. M.; Sargeson, A. M. *J. Am. Chem. Soc.* **1969**, *91*, 4102–4110. (i) Suh, J. *Acc. Chem. Res.* **1992**, *25*, 273–278. (j) Chin, J. *Acc. Chem. Res.* **1991**, *24*, 145–152.

(21) For examples of other artificial metalloproteins and metalloenzymes, see: (a) Sasaki, T.; Kaiser, T. E. *Biopolymers* **1990**, *29*, 79–88. (b) Handel, T.; DeGrado, W. F. *J. Am. Chem. Soc.* **1990**, *112*, 6710–6712. (c) Regan, L.; Clarke, N. D. *Biochemistry* **1990**, *29*, 10878–10883. (d) Braxton, S.; Wells, J. A. *Biochemistry* **1992**, *31*, 7796–7801. (e) Higaki, J. N.; Fletterick, R. J.; Craik, C. S. *Trends Biochem. Sci.* **1992**, *17*, 100–104. (f) Mack, D. P.; Dervan, P. B. *Biochemistry* **1992**, *31*, 9399–9405. (g) Ghadiri, M. R.; Soares, C.; Choi, C. *J. Am. Chem. Soc.* **1992**, *114*, 4000–4002. (h) Desjarlais, J. R.; Berg, J. M. *Proc. Natl. Acad. Sci. U.S.A.* **1993**, *90*, 2256–2260. (i) Pessi, A.; Bianchi, E.; Cramer, A.; Venturini, S.; Tramotano, A.; Sollazzo, M. *Nature* **1993**, *362*, 367–369. (j) McGrath, M. E.; Haymore, B. L.; Summers, N. L.; Craik, C. S.; Fletterick, R. J. *Biochemistry* **1993**, *32*, 1914–1919. (k) Wade, W. S.; Koh, J. S.; Han, N.; Hoekstra, D. M.; Lerner, R. A. *J. Am. Chem. Soc.* **1993**, *115*, 4449–4456. (l) Cuenoud, B.; Schepartz, A. *Science* **1993**, *259*, 510–513. (m) Bryson, J. W.; Betz, S. F.; Lu, H. S.; Suich, D. J.; Zhou, H. X.; O'Neil, K. T.; DeGrado, W. F. *Science* **1995**, *270*, 935–941.

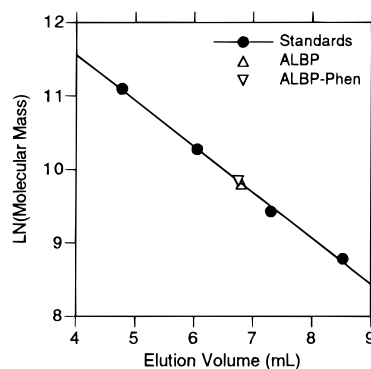
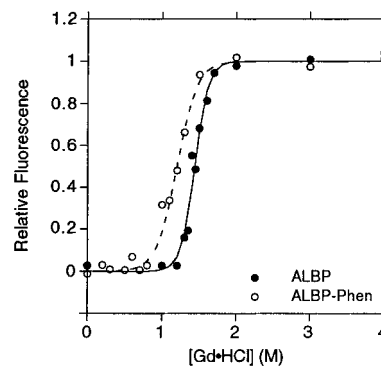
(22) Kraulis, P. J. *J. Appl. Crystallogr.* **1991**, *24*, 946–956.

Table 1. Properties of ALBP and ALBP-Phen

property	ALBP	ALBP-Phen
titratable thiols (from DTNB titration)	0.95 thiol/mol	0.10 thiol/mol
molecular mass (from electrospray MS)	14,541.59 ± 1.75 Da	14777.04 ± 2.78 Da
λ_{\max} , ϵ (from UV/vis spectroscopy)	280 nm, 17 mM ⁻¹ ·cm ⁻¹	274 nm, 29 mM ⁻¹ ·cm ⁻¹
molecular mass (from gel filtration)	19 600 Da	18 900 Da
denaturation midpoint ([guanidine·HCl])	1.4 M	1.2 M

**Figure 2.** UV/vis spectra of ALBP, ALBP-Phen, and phenanthroline: (A) spectrum of ALBP (6.5 μ M); (B) spectrum of ALBP-Phen (6.5 μ M); (C) spectrum of 1,10-phenanthroline, and (D) difference spectrum of ALBP-Phen minus ALBP.**Figure 3.** Fluorescence emission spectra of ALBP and ALBP-Phen: (A) spectrum of ALBP (1.0 μ M) and (B) spectrum of ALBP-Phen (1.0 μ M). Spectra were obtained by excitation at 275 nm.

ALBP results in a shift in λ_{\max} from 280 to 274 nm accompanied by a substantial increase in extinction. Subtraction of these two spectra leads to a difference spectrum (D) that is similar to the spectrum of unsubstituted 1,10-phenanthroline (C). Figure 3 shows fluorescence emission spectra for ALBP (A) and ALBP-Phen (B). An emission maximum at 406 nm appears only in the spectrum of ALBP-Phen and can be attributed to the phenanthroline fluorophore. It is also interesting to note that the tryptophan fluorescence centered at 340 nm in ALBP is substantially reduced in ALBP-Phen; this is likely due to quenching by the phenanthroline. Additional evidence for phenanthroline attachment derives from electron spray ionization mass spectrometry. Spectra obtained from samples of ALBP and ALBP-Phen gave masses of 14 541.59 (\pm 1.75) Da and 14 777.04 (\pm 2.78) Da, respectively. These results give an observed mass difference of 235.45 Da that is in close agreement with the calculated mass difference of 235 Da attributable to the phenanthroline moiety. Gel filtration chromatography was performed on samples of ALBP and ALBP-Phen under non-denaturing conditions, and the apparent masses of the proteins were estimated by comparing their elution volumes with those from a set of standard proteins (Figure 4). ALBP and ALBP-Phen gave masses of 19 600 and 18 900 Da. The similarity of these values suggests that ALBP and ALBP-Phen have com-

**Figure 4.** Gel filtration molecular mass analysis of ALBP-Phen: (●) standards, (Δ) ALBP, and (∇) ALBP-Phen.**Figure 5.** Guanidine hydrochloride denaturation profiles for ALBP and ALBP-Phen obtained by fluorescence spectroscopy: (●) ALBP and (○) ALBP-Phen.

parable folded structures; no large perturbations of the ALBP structure occur upon alkylation with **1**. It should be noted that the masses for both proteins obtained by gel filtration chromatography differ from those determined by mass spectrometry and denaturing electrophoresis (data not shown). These differences most likely reflect the extended, largely β -sheet secondary structure of ALBP that differs from the more compact globular proteins typically used to standardize gel filtration chromatography experiments. As shown in Figure 5, denaturation experiments monitored by fluorescence spectroscopy using guanidinium chloride as a denaturant were performed to estimate the effect of phenanthroline attachment on protein stability. ALBP and ALBP-Phen gave values of 1.4 and 1.2 M, respectively, for their denaturation midpoints indicating that conjugation of ALBP with phenanthroline does not result in any large destabilization of the protein. Finally, it should also be noted that titration of ALBP-Phen with the fluorescent fatty acid analogs *cis*-paranaric acid and 12-anthroloxyoleic acid indicate that the conjugate lacks the ability to bind fatty acids. These results are similar to those observed by Bernlohr and co-workers who have previously reported that modification of Cys₁₁₇ with a number of agents greatly attenuates fatty acid binding to ALBP.^{14c,d}

Copper Binding to ALBP-Phen. The binding of Cu(II) to ALBP-Phen was first examined by fluorescence measurements. As shown in Figure 6, addition of Cu(II) to a solution containing

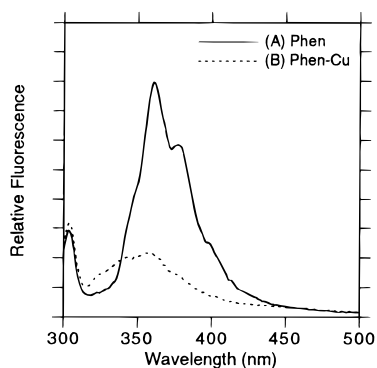


Figure 6. 1,10-Phenanthroline fluorescence quenching by Cu(II). Fluorescence emission spectra of (A) 1,10-phenanthroline and (B) 1,10-phenanthroline in the presence of 2 equivs of Cu(II).

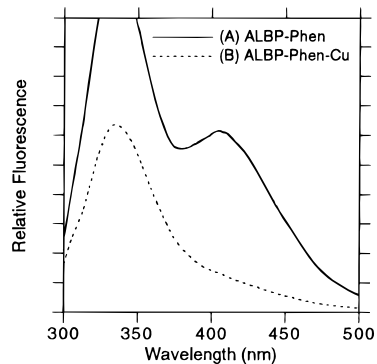


Figure 7. Phenanthroline fluorescence quenching by Cu(II) in ALBP-Phen. Fluorescence emission spectra of (A) ALBP-Phen and (B) ALBP-Phen in the presence of 40 equivs of Cu(II).

phenanthroline (A) resulted in substantial quenching of the phenanthroline fluorescence (B). Figure 7 shows a similar experiment with ALBP-Phen. Addition of Cu(II) to a sample of ALBP-Phen (A) resulted in quenching of the phenanthroline fluorescence (B); several equivs of Cu(II) were necessary to drive this reaction to completion. This may reflect the fact that the ALBP cavity is lined with several cationic residues that are involved in fatty acid binding which may repel the entry of the additional cations. Treatment of ALBP-Phen with Cu(II) followed by gel filtration to remove unbound metal ions resulted in a sample whose phenanthroline fluorescence remained quenched upon prolonged storage and suggested that Cu(II) remains bound and is not subject to loss over several weeks.

Although the above experiments suggested that Cu(II) remained bound to ALBP-Phen for prolonged periods of time in the absence of competing ligands free in solution, it was also important to analyze the stability of this complex in the presence of exogenous ligands. Thus the phenanthroline-Cu(II) and ALBP-Phen-Cu(II) complexes were examined in the presence of EDTA, picolinic acid, and alanine. Addition of EDTA to solutions of phenanthroline-Cu(II) and ALBP-Phen-Cu(II) resulted in the return of phenanthroline fluorescence indicating that Cu(II) was being removed by this powerful chelating agent (data not shown). In contrast, addition of picolinate or alanine gave significantly different results. As shown in Figure 8A, in PIPES buffer (pH 6.1), the fluorescence of phenanthroline is quenched by Cu(II), but this effect can be partially reversed by the addition of picolinate. As shown in Figure 8B, titration of phenanthroline-Cu(II) with up to 4 equivs of picolinate results in the return of approximately half of the phenanthroline fluorescence. These results are in contrast to those obtained with EDTA shown in Figure 9A. Clearly, picolinate is less effective than EDTA at removing the Cu(II). Figure 9B shows

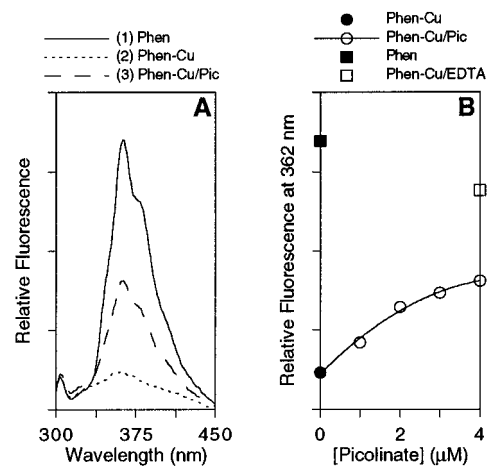


Figure 8. Fluorescence of 1,10-phenanthroline-Cu(II) in the presence of picolinic acid. (A) Emission spectra of 1,10-phenanthroline (1), 1,10-phenanthroline-Cu(II) (2), and 1,10-phenanthroline-Cu(II) in the presence of 4 equivs of picolinic acid (3). (B) Fluorescence at 362 nm of 1,10-phenanthroline-Cu(II) in the absence (●) and presence (○) of picolinate. The fluorescence of 1,10-phenanthroline is indicated by (■), and the fluorescence of 1,10-phenanthroline-Cu(II) following the addition of EDTA is given by (□).

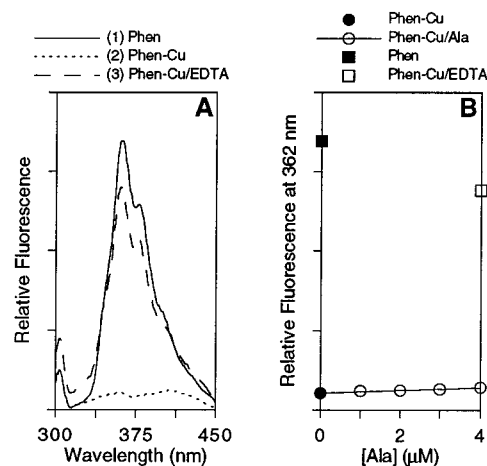


Figure 9. Fluorescence of 1,10-phenanthroline-Cu(II) in the presence of alanine. (A) Emission spectra of 1,10-phenanthroline (1), 1,10-phenanthroline-Cu(II) (2), and 1,10-phenanthroline-Cu(II) in the presence of excess EDTA (3). (B) Fluorescence at 362 nm of 1,10-phenanthroline-Cu(II) in the absence (●) and presence (m) of alanine. The fluorescence of 1,10-phenanthroline is indicated by (■), and the fluorescence of 1,10-phenanthroline-Cu(II) following the addition of EDTA is given by (□).

that titration of phenanthroline-Cu(II) with alanine results in only a small return in phenanthroline fluorescence even after the addition of several equivalents. Thus, alanine is less effective than picolinic acid at removing the Cu(II) from phenanthroline.

Experiments similar to those described above were also performed with samples of ALBP-Phen-Cu(II). However, in these cases, significantly different results were obtained. Titration of ALBP-Phen-Cu(II) with picolinic acid, shown in Figure 10A, results in a decrease in the protein fluorescence at 336 nm, but no change in the phenanthroline fluorescence at 406 nm. In fact, Figure 10B shows that the 406 nm fluorescence does not increase even after the addition of 4 equivs of picolinate although there is an immediate increase upon addition of EDTA. The decrease in protein fluorescence at 336 nm suggests that picolinic acid is binding to the protein although the nature of this complex remains undefined; picolinate may or may not be

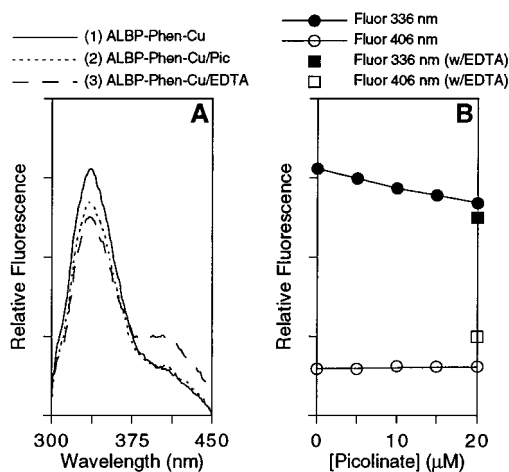
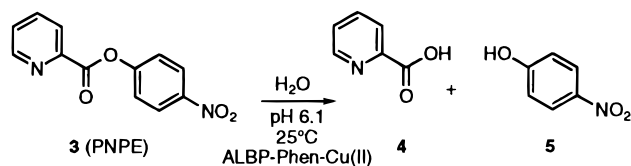


Figure 10. Fluorescence of ALBP-Phen-Cu(II) in the presence of picolinic acid. (A) Emission spectra of ALBP-Phen-Cu(II) (1), ALBP-Phen-Cu(II) in the presence of 4 equivs of picolinic acid (2), and ALBP-Phen-Cu(II) in the presence of excess EDTA (3). (B) Fluorescence at 336 nm (●) and 406 nm (○) of ALBP-Phen-Cu(II) in the presence of picolinate. The fluorescence at 336 nm (■) and 406 nm (□) of ALBP-Phen-Cu(II) upon the addition of excess EDTA.

bound to Cu(II). Nevertheless, it is clear that Cu(II) remains bound to the phenanthroline in the presence of excess picolinate. Similar results were obtained upon titration of ALBP-Phen-Cu(II) with alanine. As shown in Figure 11A,B, a small diminution in the 336 nm fluorescence is observed upon addition of alanine, but no increase in 406 nm fluorescence occurs. Thus, in contrast to phenanthroline-Cu(II), ALBP-Phen-Cu(II) does not appear to release Cu(II) in the presence of picolinate or alanine.

Activated Ester Hydrolysis. With a well characterized conjugate in hand, the ability of ALBP-Phen-Cu(II) to hydrolyze an activated ester substrate was examined; the bidentate ligand/substrate picolinic acid nitrophenyl ester (PNPE) was employed in this study since the production of nitrophenol (**5**) could be followed spectrophotometrically. Hydrolysis reactions were



performed with excess **3** in PIPES buffer, pH 6.1, at 25 °C. Incubation of ALBP-Phen-Cu(II) with **3** resulted in the hydrolysis of at least 2 equivs of **3** in 2 h. As shown in Figure 12, the rate of hydrolysis for the ALBP-Phen-Cu(II)-containing reaction is 5-fold greater than the background hydrolysis rate and is linear over 6 h (6 turnovers, data not shown). In contrast, Figure 12 also shows that reactions containing free Cu(II) give biphasic progress curves.^{18b} In the early part of the reaction, 1 equiv of **3** is hydrolyzed rapidly. This is followed by a decrease in the hydrolysis rate to that of the background rate. The rapid phase of the reaction is likely due to the hydrolysis of **3** bound to free Cu(II), while the slow phase is attributable to hydrolysis of **3** promoted by a picolinate-Cu(II) complex or simply background hydrolysis. Thus, these experiments demonstrate that ALBP-Phen-Cu(II), but not free Cu(II), can promote the catalytic hydrolysis of PNPE with a modest (5-fold) increase in rate relative to background. However, because of the high rates for the background reaction, this substrate was not studied further.

Stereoselective Ester Hydrolysis. To obtain a lower rate for background hydrolysis, unactivated alkyl esters of amino

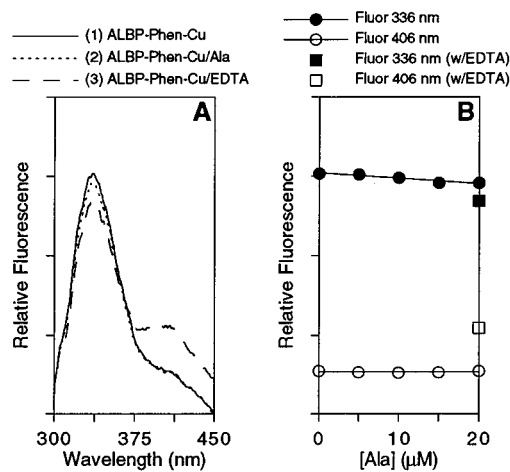


Figure 11. Fluorescence of ALBP-Phen-Cu(II) in the presence of alanine. (A) Emission spectra of ALBP-Phen-Cu(II) (1), ALBP-Phen-Cu(II) in the presence of 4 equivs of alanine (2), and ALBP-Phen-Cu(II) in the presence of excess EDTA (3). (B) Fluorescence at 336 nm (●) and 406 nm (○) of ALBP-Phen-Cu(II) in the presence of alanine. The fluorescence at 336 nm (■) and 406 nm (□) of ALBP-Phen-Cu(II) upon the addition of excess EDTA.

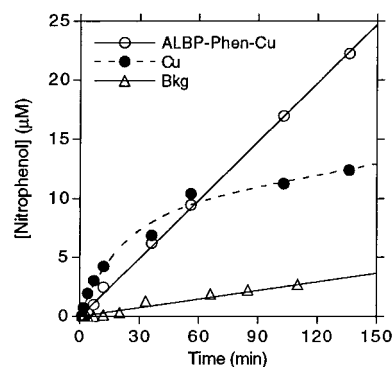
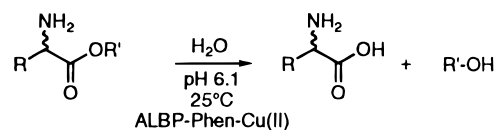


Figure 12. Hydrolysis of PNPE (**3**) by ALBP-Phen-Cu(II) and Cu(II). Concentration of *p*-nitrophenol (**5**) produced by 10 μM ALBP-Phen-Cu(II) (○), 10 μM Cu(II) (●) or buffer alone (△).

acid substrates were studied next. These compounds also allowed the enantioselectivity of hydrolysis catalyzed by ALBP-Phen-Cu(II) to be assessed; data for these experiments are



- | | |
|--|--|
| 6a R = CH ₃ , R' = CH ₃ | 7 R = CH ₃ |
| 6b R = CH ₃ , R' = CH ₃ CH ₂ | |
| 6c R = CH ₃ , R' = (CH ₃) ₂ CH | |
| 8a R = HOC ₆ H ₅ CH ₂ , R' = CH ₃ | 9 R = HOC ₆ H ₄ CH ₂ |
| 8b R = HOC ₆ H ₄ CH ₂ , R' = CH ₃ CH ₂ | |
| 10 R = HOCH ₂ , R' = CH ₃ | 11 R = HOCH ₂ |

tabulated in Table 2. Hydrolysis reactions were performed with racemic amino acid esters in PIPES buffer, pH 6.1, at 25 °C and monitored by derivatizing the amino acid products with *o*-phthalaldehyde and *N*-acetyl-L-cysteine. The resulting diastereomers were separated by reversed phase HPLC and quantified by fluorescence detection.²³ A chromatogram showing the separation of the two diastereomeric alanine derivatives is shown in Figure 13A. Reaction of ALBP-Phen-Cu(II) with

(23) (a) Nimura, N.; Kinoshita, T. *J. Chromatogr.* **1986**, *352*, 169–177. (b) Buck, R. H.; Krummen, K. *J. Chromatogr.* **1987**, *387*, 255–265. (c) Koh, J. T. L. D.; Breslow, R. *J. Am. Chem. Soc.* **1994**, *116*, 11234–11240.

Table 2. Kinetic Data for the Hydrolysis of Amino Acid Esters Catalyzed by ALBP-Phen-Cu(II)

substrate	temp (°C)	turnovers (n)	ee (%)	$k_{\text{cat(D)}} (M^{-1}\cdot s^{-1})$	$k_{\text{cat(L)}} (M^{-1}\cdot s^{-1})$	$k_{\text{cat(T)}} (M^{-1}\cdot s^{-1})$	$k_{\text{uncat}} (M^{-1}\cdot s^{-1})$	$k_{\text{cat(T)}/k_{\text{uncat}}}$
Ala-OMe, 3a	25	5.5	67 ± 6.0	8.5 (±2.9) × 10 ²	4.2 (±1.6) × 10 ³	5.1 × 10 ³	7.5 (±1.5) × 10 ¹	68
Ala-OEt, 3b	25	3.0	40 ± 5.0	8.3 (±2.1) × 10 ²	1.9 (±0.43) × 10 ³	2.8 × 10 ³	2.7 (±0.23) × 10 ¹	110
Ala-OiPr, 3c	25	1.3	86 ± 9.0	8.8 (±5.3) × 10 ¹	1.2 (±0.38) × 10 ³	1.2 × 10 ³	0.93 (±2.3) × 10 ¹	130
Tyr-OMe, 5a	25	7.6	39 ± 4.0	2.1 (±0.34) × 10 ³	4.9 (±0.48) × 10 ³	7.0 × 10 ³	2.5 (±0.31) × 10 ¹	280
Tyr-OMe, 5a	15	1.3	79 ± 2.0	1.2 (±0.18) × 10 ²	1.1 (±0.03) × 10 ³	1.2 × 10 ³	1.9 (±0.31) × 10 ¹	61
Tyr-OMe, 5a	4	0.70	86 ± 8.0	4.4 (±2.7) × 10 ¹	6.0 (±0.03) × 10 ²	6.4 × 10 ²	1.5 (±0.08) × 10 ¹	44
Tyr-OEt, 5b	25	0.70	31 ± 11	2.3 (±0.71) × 10 ²	4.3 (±0.71) × 10 ²	6.6 × 10 ²	2.1 (±0.11) × 10 ¹	32
Ser-OMe, 7	25	2.3	43 ± 1.3	1.5 (±0.02) × 10 ³	6.2 (±0.19) × 10 ²	2.1 × 10 ³	4.4 (±0.34) × 10 ¹	48
PMNA, 9	37	0.7				3.6 × 10 ²	2.3 × 10 ⁻²	1.6 × 10 ⁴

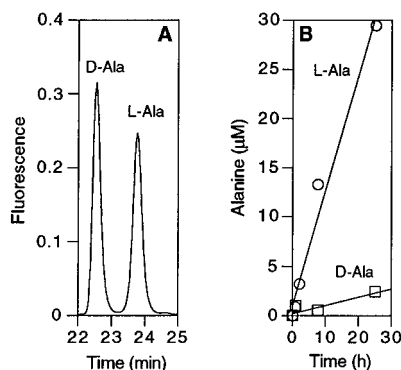
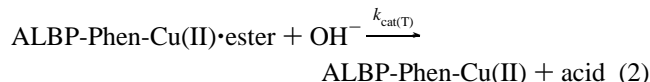
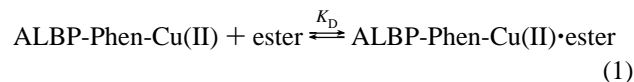


Figure 13. Hydrolysis of a racemic mixture of alanine isopropyl ester is selective for the L enantiomer. Panel A: Reversed-phase HPLC chromatogram showing the separation of diastereomeric derivatives prepared from a racemic mixture of alanine. Panel B: Rates of hydrolysis of the two enantiomers of alanine isopropyl ester catalyzed by ALBP-Phen-Cu(II).

alanine ethyl ester (**6b**) over a 24 h period gave a linear rate for the production of alanine; after 24 h the conjugate had catalyzed the hydrolysis of 3 equivs of the ester substrate. Interestingly, modest stereoselectivity was observed in this reaction. The L enantiomer was hydrolyzed 2.3 times faster than the D isomer. Better selectivity was obtained with the bulkier substrate alanine isopropyl ester (**6c**). In this case the L enantiomer was hydrolyzed 13 times faster (see Figure 13B) than the D isomer with 1.3 equivs of alanine produced in 24 h. The corresponding L enantiomer of alanine methyl ester (**6a**) was hydrolyzed 5 times faster than the D ester and produced 5.5 equivs of alanine in 24 h. Other amino acid esters can be hydrolyzed by ALBP-Phen as well. The L isomer of tyrosine ethyl ester (**8b**) was hydrolyzed 1.9 times more rapidly than the D enantiomer; in this case 0.7 equivs were hydrolyzed in 24 h. The L enantiomer of tyrosine methyl ester (**8a**) underwent hydrolysis 2.3 times faster than the D enantiomer giving 7.6 equivs of tyrosine (**9**) in 24 h. This selectivity increased at lower temperature. At 15 °C, the L enantiomer of **8a** hydrolyzed 8.6 times faster than the D isomer, and at 4 °C the selectivity for the L enantiomer increased to 14-fold above that for the D enantiomer. However, this increase in selectivity was accompanied by a decrease in overall conversion. At 15 °C, 1.3 equivs of **8a** were hydrolyzed, and at 4 °C only 0.7 equivs were hydrolyzed. Serine methyl ester (**9a**) was also hydrolyzed by ALBP-Phen, but with the opposite stereoselectivity. In this case, 2.3 equivs of **9a** were hydrolyzed in 24 h by the conjugate with the D enantiomer reacting 2.4 times more rapidly than the L isomer. Interestingly, all attempts to hydrolyze valine esters were unsuccessful with no reaction being observed for either the methyl, ethyl, or isopropyl esters.

The rates for ester hydrolysis reactions catalyzed by ALBP-Phen-Cu(II) were next analyzed using the kinetic scheme shown below



In this mechanism, an ester substrate binds to ALBP-Phen-Cu(II) to form a complex that then reacts with OH⁻ to form the acid product. Using a rapid equilibrium approach, the following equation for the rate can be written

$$\frac{d[\text{acid}]_{\text{cat}}}{dt} = \frac{k_{\text{cat(T)}}[\text{ALBP-Phen-Cu(II)}][\text{ester}][\text{OH}^-]}{K_D + [\text{ester}]} \quad (3)$$

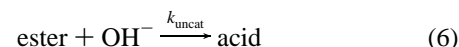
This expression can be simplified when [ester] ≫ K_D. Given the concentration of ester present in these reactions (1 mM) and the known dissociation constants for Cu(II) amino acid ester complexes (ca. 100 μM), this is a reasonable assumption.²⁴ Thus (3) can be reduced as follows:

$$\frac{d[\text{acid}]_{\text{cat}}}{dt} = k_{\text{cat(T)}}[\text{ALBP-Phen-Cu(II)}][\text{OH}^-] \quad (4)$$

The term $k_{\text{cat(T)}}$ can be viewed as the sum of the rate constants for the hydrolysis of the two enantiomeric amino acid esters

$$k_{\text{cat(T)}} = k_{\text{cat(D)}} + k_{\text{cat(L)}} \quad (5)$$

The uncatalyzed background reaction is shown below



An equation for the background reaction rate can also be written

$$\frac{d[\text{acid}]}{dt} = k_{\text{uncat}}[\text{ester}][\text{OH}^-] \quad (7)$$

Using eqs 4, 5, and 7, the second order rate constants for amino acid ester hydrolysis in the presence and absence of ALBP-Phen-Cu(II) were calculated and are listed in Table 2. Values for $k_{\text{cat(T)}}$ range from 6.4×10^4 – $7.0 \times 10^3 \text{ M}^{-1}\cdot\text{s}^{-1}$, while k_{uncat} values vary from 9.3 to $75 \text{ M}^{-1}\cdot\text{s}^{-1}$. Calculation of the ratio $k_{\text{cat(T)}/k_{\text{uncat}}}$ for the various amino acid ester hydrolysis reactions gives values ranging from 32 to 280 and provides an indication of the relative rate enhancement resulting from the ALBP-Phen-Cu(II) catalyst.

Amide Hydrolysis. The ability of ALBP-Phen-Cu(II) to hydrolyze amide bonds was examined next using the substrate picolinic acid nitromethyl anilide (PMNA, **12**). This compound produces *N*-methyl-4-nitroaniline (MNA, **13**) upon hydrolysis which can be monitored spectrophotometrically at 400 nm.

(24) See: Nakon, R.; Rechani, P. R.; Angelici, R. J. *J. Am. Chem. Soc.* **1974**, *96*, 2117–2120, and references therein.

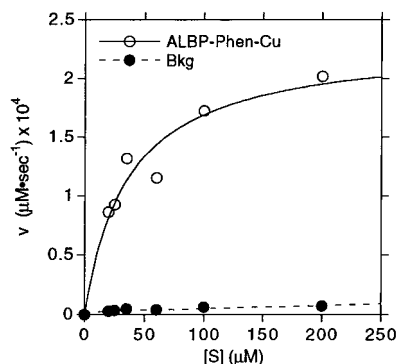


Figure 14. Rate versus substrate concentration profile of ALBP-Phen-Cu(II) promoted PMNA hydrolysis. Saturation kinetics is observed with ALBP-Phen-Cu(II) (○), while the background rate of PMNA hydrolysis (●) increases linearly with increasing concentrations of PMNA.

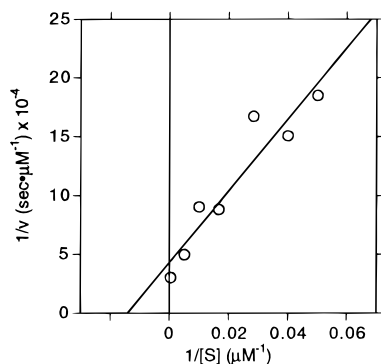
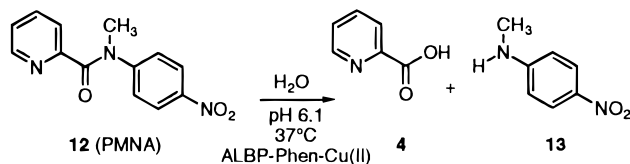


Figure 15. Double reciprocal analysis of ALBP-Phen-Cu(II) promoted PMNA (**12**) hydrolysis. Plot of the reciprocal of the initial rate of NMA (**13**) formation ($1/v$) versus the reciprocal of [PMNA] ($1/[S]$) catalyzed by ALBP-Phen-Cu(II).



ALBP-Phen-Cu(II) was incubated with PMNA in PIPES buffer, pH 6.1, at 37 °C, and the rate of *N*-methyl-4-nitroaniline production was determined. These experiments demonstrated that ALBP-Phen-Cu(II) was capable of hydrolyzing an aryl amide bond. It should be noted that only low levels of background hydrolysis were observed using ALBP instead of ALBP-Phen-Cu(II) as a catalyst. Analysis of initial rate data at various PMNA concentrations, illustrated in Figure 14, shows that ALBP-Phen-Cu(II) catalyzed PMNA hydrolysis exhibits saturation kinetics, while the background rate of PMNA hydrolysis (which is quite low) increases linearly with increasing concentrations of PMNA up to 200 μM ; thus, this saturation phenomenon is not due to a solubility effect. The ALBP-Phen-Cu(II) catalyzed PMNA hydrolysis is consistent with the rate law given below

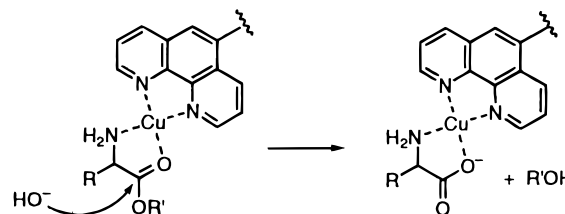
$$\frac{d[\text{MNA}]_{\text{cat}}}{dt} = \frac{k_{\text{cat}}[\text{ALBP-Phen-Cu(II)}][\text{PMNA}][\text{OH}^-]}{K_D + [\text{PMNA}]} \quad (8)$$

A double reciprocal plot of the rate data showing this “enzyme-like” behavior is given in Figure 15. Further analysis of these data gave values of 70 μM for K_D and 360 $\text{M}^{-1}\cdot\text{s}^{-1}$ for k_{cat} . Using a published value for k_{uncat} of $2.3 \times 10^{-2} \text{M}^{-1}\cdot\text{s}^{-1}$, a value of 1.6×10^4 was calculated for the ratio $k_{\text{cat}}/k_{\text{uncat}}$.^{19b}

Discussion

The conjugate ALBP-Phen was prepared by alkylation of a unique cysteine residue (Cys₁₁₇) from ALBP with iodoaceto-mido-1,10-phenanthroline. Thiol titration data confirms that Cys₁₁₇ has been modified. UV/vis spectroscopy, fluorescence measurements, and electrospray mass spectrometry indicate that a covalently bound phenanthroline moiety is present. Gel filtration and guanidine denaturation experiments suggest that the overall ALBP structure remains intact. Fluorescence and UV/vis measurements are consistent with Cu(II) bound to the phenanthroline. Taken together, these data provide compelling evidence for the preparation of the desired conjugate, ALBP-Phen.

The conjugate ALBP-Phen-Cu(II) provides a metal binding site within a well defined protein cavity. This sequestered Cu(II) ion catalyzes the hydrolysis of *unactivated* esters and amides at neutral pH. A possible mechanism for ALBP-Phen-Cu(II) promoted ester hydrolysis is shown below. This mechanism is presented only to give a picture of what may be occurring with ALBP-Phen-Cu(II); alternative mechanisms can be envisioned. For ester substrates, several amino acid esters including alanine,



serine, and tyrosine can be hydrolyzed. However, the β -branched amino acid valine ethyl ester is not a substrate. In all cases the hydrolytic reactions are stereoselective and produce the *L* isomers (except for serine) with modest selectivity. The selectivities obtained depend on the amino acid and type of alkoxy group present in the substrate; the enantioselectivity for alanine isopropyl ester hydrolysis is much greater than that for the corresponding ethyl ester (40% versus 86% *ee*). Efficient hydrolysis of tyrosine methyl ester occurs at temperatures as low as 4 °C which results in a concomitant increase in selectivity (39% *ee* at 25 °C, 86% *ee* at 4 °C). The second order rate constants for ester hydrolysis ($k_{\text{cat(T)}}$) vary from 6.4×10^2 – $7.0 \times 10^3 \text{M}^{-1}\cdot\text{s}^{-1}$ (Table 2) and are comparable to those observed by Angelici and co-workers for Cu(II) promoted glycine methyl ester hydrolysis. Specifically, the values for $k_{\text{cat(T)}}$ reported here are less than those obtained by Nakon *et al.* with uncomplexed Cu(II) ($k_{\text{cat(T)}} = 7.6 \times 10^4 \text{M}^{-1}\cdot\text{s}^{-1}$) but higher than those obtained with Cu(II)·(nitrilotriacetic acid) ($k_{\text{cat(T)}} = 4.6 \times 10^2 \text{M}^{-1}\cdot\text{s}^{-1}$).^{19e} The attenuated hydrolysis rate constants obtained in the presence of ligands such as ALBP-Phen probably reflect the decreased Lewis acidity of the phenanthroline-coordinated Cu(II) relative to that of free Cu(II).

PMNA, an amide containing substrate, is also hydrolyzed by ALBP-Phen-Cu(II) although this reaction requires higher temperatures (37 °C) and longer incubation times (several days). The initial rates of hydrolysis exhibit saturation kinetics consistent with enzymatic behavior. Analysis of these rate data gave values for K_D (70 μM) and k_{cat} (360 $\text{M}^{-1}\cdot\text{s}^{-1}$). The value of k_{cat} obtained with ALBP-Phen-Cu(II) is 67-fold lower than the corresponding value obtained with Cu(II)·(2,2'-bipyridine) by Sayre and co-workers at 40 °C in EtOH/H₂O although there is still considerable rate acceleration ($k_{\text{cat}}/k_{\text{uncat}} = 1.6 \times 10^4$).^{19a} This decrease in rate may reflect a nonoptimal geometry for PMNA binding within the ALBP cavity due to steric interactions. It is also interesting to compare the K_D value of 70 μM

obtained with ALBP-Phen-Cu(II) to the value for K_D of "greater than 10 mM" estimated by Reddy *et al.* for Cu(II)•(2,2'-bipyridine) catalyzed PMNA hydrolysis.^{19b} Clearly, the hydrophobic cavity of the ALBP protein is enhancing the binding of PMNA to the bound Cu(II) although not to the same extent that it does for fatty acids since the K_D values for these physiologically relevant ligands are below 1 μ M.

An important issue related to the chemistry reported here concerns the question of whether or not our results can be attributed to the presence of small amounts of free Cu(II) in our reactions. We believe that this is not the case for three reasons. First, fluorescence experiments with ALBP-Phen-Cu(II) showed that the addition of picolinate or alanine did not lead to measurable decomplexation of Cu(II) even in the presence of excess ligand after 24 h of incubation. However, it is interesting to note that, in similar experiments, picolinate and alanine (to a small extent) were able to remove Cu(II) from free phenanthroline. Thus, the cupric ion present in ALBP-Phen-Cu(II) is clearly in a sequestered environment more characteristic of protein-bound metal ions. Second, the hydrolysis of amino acid esters reported here occurred in an enantioselective manner. This would not be possible if free Cu(II) was the actual catalyst. For the achiral substrates (**3** and **12**), a third line of reasoning can be considered. Initial experiments with picolinic acid nitrophenyl ester (**3**) showed that while free Cu(II) promoted the hydrolysis of 1 equiv of substrate more rapidly than ALBP-Phen-Cu(II), Cu(II) did not effect catalytic hydrolysis; the rate of hydrolysis of **3** after one turnover was close to or equal to that of the background reaction. This observation is consistent with results reported by other investigators and can be attributed to the lower reactivity of the picolinate-Cu(II) complex whose Lewis acidity has been attenuated by the negatively charged picolinate ligand. Thus, the catalytic hydrolysis of **3** cannot be accounted for by the presence of free Cu(II). Similar reasoning can be used to rule out the involvement of free Cu(II) in the amide hydrolysis reactions. Although catalytic hydrolysis of **12** was not observed with ALBP-Phen-Cu(II), it was possible to detect the hydrolysis of 0.7 equivs of substrate. Since decomplexation of 70% of ALBP-Phen-Cu(II) would have been detected in our fluorescence experiments, this hydrolysis could not result from a large amount of free Cu(II). However, if this reaction involved a trace of free Cu(II) acting in a catalytic fashion, the active species would have to be a picolinate-Cu(II) complex. As noted above, such a complex is actually less reactive in ester hydrolysis than ALBP-Phen-Cu(II).

As a final note, it should be pointed out that the hydrolysis rates described here are reported relative to the rates of background hydrolysis in the absence of Cu(II). This was done in lieu of reporting the rates relative to free Cu(II) or phenanthroline-Cu(II) since the former is not present under catalytic conditions (after one turnover it gains a ligand), whereas the latter undergoes ligand exchange with the reaction products to varying extents. Moreover, since one of the goals of our work in this area is to develop selective protein-based catalysts, the ratio of the rate of the protein-catalyzed reaction versus the background rate is of particular importance. The enantioselectivity that can be obtained in a kinetic resolution reaction is, in part, controlled by this ratio. However, it is still useful to note that the rate enhancements for ester and amide hydrolysis reported here are 10^2 – 10^3 lower than those observed for free Cu(II) (under single turnover conditions) but comparable to those previously reported for Cu(II) complexes.^{19c} Thus, introduction of the phenanthroline-Cu(II) moiety into ALBP does not substantially alter the reactivity of the metal complex.

This is not surprising given the fact that the protein does not contribute additional ligands or functional groups that could participate in general acid/base chemistry; the cavity is primarily a hydrophobic, shape-selective pocket that can only control the reaction specificity. Efforts to introduce additional side chains via mutagenesis to modulate the reactivity and specificity are currently underway.

The selectivity and catalytic properties of ALBP-Phen clearly demonstrate that covalent modification of the ALBP cavity can be used to generate a metal ion-containing hydrolytic catalyst with enzyme-like features. Although the efficiency and selectivity exhibited by this construct are significantly less than those of naturally occurring enzymes, the ALBP cavity portends to be a useful system for the development of new catalysts. Several other conjugates have already been prepared which perform reactions with selectivities as high as 95% *ee*.¹² Mutants have been prepared that alter the catalytic efficiency and selectivity of transformations performed in the cavity.²⁵ Finally, crystals of several ALBP conjugates, including ALBP-Phen, suitable for X-ray analysis have been prepared and are being studied to provide a structural framework for understanding the selectivities of reactions that have been carried out within this constrained protein cavity.²⁶

Experimental Section

General Instrumentation and Materials. Fluorescence measurements were performed with a Perkin Elmer Luminescence Spectrometer LS 50B, and UV data were obtained using a Hewlett Packard Diode Array Spectrophotometer 8452A. Iodoacetamido-1,10-phenanthroline²⁷ (**1**), picolinic acid *p*-nitrophenyl ester (**3**), and picolinic acid methyl-nitroanilide^{19a} (**12**) were synthesized according to published procedures. Amino acid esters were purchased from Aldrich or were prepared from the corresponding amino acids by standard methods. *E. coli* JM105/pMON4 was a generous gift from Dr. D. Bernlohr, Department of Biochemistry, University of Minnesota, Minneapolis, MN, 55455.

Purification of ALBP. Cultures of *E. coli* JM105/pMON4 were grown in LB media (4 \times 1L) to an OD₆₀₀ of 0.8, induced with nalidixic acid, and grown for an additional 4 h. The cells were then harvested by centrifugation, frozen in N₂(l), and stored at -80 °C until purification. The frozen cell paste (21 g) was resuspended in 50 mL of buffer A (25 mM imidazole-HCl, pH 7.0, 50 mM NaCl, 5 mM EDTA, 0.1 mM PMSF, and 1 mM 2-mercaptoethanol). The cells were then lysed by sonication (0 °C, 5 min), and the cellular debris was removed by centrifugation. Protamine sulfate (5 mL, 5% in Buffer A) was added dropwise to the supernatant at 4 °C, and the cloudy mixture was stirred for another 45 min. The precipitate was removed by centrifugation. The supernatant was titrated to pH 5.0 with sodium acetate (2.0 M, pH 4.9), and the mixture was allowed to stir overnight at 4 °C. The supernatant was clarified by centrifugation and was concentrated to 7 mL by ultrafiltration (YM3 filters, Amicon). The concentrated protein solution was fractionated by chromatography employing a Sephadex G-75 Superfine column (5 cm \times 100 cm) equilibrated in buffer B (12.5 mM HEPES, pH 7.2, and 0.25 M NaCl) and eluted at 0.5 mL/min. The ALBP eluted after approximately 39 h. The fractions containing the protein were identified by SDS PAGE and concentrated by ultrafiltration. Approximately 75 mg of protein was obtained as determined by the Bradford protein assay²⁸ and UV ($\epsilon_{278} = 15\,500\text{ M}^{-1}\text{ cm}^{-1}$).²⁹ The purified ALBP was shown to be active by its ability to bind fluorescent fatty acid analogs.³⁰

(25) Kuang, H.; Davies, R. R.; Distefano, M. D. *Bioorg. Med. Chem. Lett.* **1997**, 7, 2055–2060.

(26) Ory, J.; Mazhary, A.; Kuang, H.; Davies, R. R.; Distefano, M. D.; Banaszak, L. J. Submitted.

(27) Chen, C. B.; Sigman, D. S. *Proc. Natl. Acad. Sci. U.S.A.* **1986**, 83, 7147–7150.

(28) Bradford, M. M. *Anal. Biochem.* **1976**, 72, 248–254.

(29) Buel, M. K.; Bernlohr, D. A. *Biochemistry* **1990**, 29, 7408–7413.

(30) Sha, R. S.; Kane, C. D.; Xu, Z.; Banaszak, L. J.; Bernlohr, D. A. *J. Biol. Chem.* **1993**, 268, 7885–7892.

Synthesis of ALBP-Phen. A solution of iodoacetamido-1,10-phenanthroline (100 mM) in DMF (128 μL) was added to a solution of purified ALBP (53 μM , 21.5 mL) in HEPES buffer (12.5 mM, pH 7.2), and the mixture was allowed to react at room temperature, in the dark, for approximately 48 h. The reaction was monitored by titration with 5,5'-dithiobis-(2-nitrobenzoic acid) (DTNB) in 5.2 M guanidine hydrochloride as described by Riddles et al. to determine the extent of alkylation of Cys₁₁₇.³¹ Conjugation reactions were typically 85% to 95% complete based on this assay. Following conjugation, the solution was concentrated 5-fold by ultrafiltration and purified by gel filtration chromatography (Biogel P6-DG, Biorad) in Tris·HCl (50 mM, pH 7.4) to remove the excess phenanthroline reagent. The fractions containing the purified ALBP-Phen were combined and concentrated, and the concentration of the final product was determined by protein assay.

Metallation of ALBP-Phen. CuSO₄ (1.5 mL, 10 mM, in Tris·HCl, 50 mM, pH 7.4) was added to a solution of ALBP-Phen (1.5 mL, 150 μM) in the same buffer and allowed to react for 1 h at ambient temperature. Copper binding was confirmed by fluorescence spectroscopy (as described below), and the unbound copper was removed by gel filtration chromatography (Biogel P6-DG, Biorad) in PIPES buffer (10 mM, pH 6.1).

UV/vis and Fluorescence Spectroscopy. UV/vis spectra of ALBP and ALBP-Phen were obtained using 6.5 μM protein determined by a Bradford protein assay in 25 mM Tris, pH 7.4. UV data for 1,10-phenanthroline was obtained in the same buffer. Fluorescence spectra for ALBP and ALBP-Phen were obtained in 50 mM Tris, pH 7.4. To follow ALBP-Phen metallation, the fluorescence of a solution of ALBP-Phen (1.0 mL, 1.0 μM) in Tris·HCl (50 mM, pH 7.4) was obtained, and CuSO₄ (1.0 mM in Tris buffer) was titrated into the solution (40 μL total) until there was no further change in the phenanthroline fluorescence ($\lambda_{\text{ex}} = 275 \text{ nm}$, $\lambda_{\text{em}} = 406 \text{ nm}$). The excess copper was then removed by gel filtration (NAP 10 column, Pharmacia), and the fluorescence spectrum was again obtained. A similar procedure was performed with 1,10-phenanthroline; however, only 2 equivs of CuSO₄ were needed to completely quench the fluorescence. Ligand competition experiments between phenanthroline-Cu(II) and picolinate or alanine were performed using phenanthroline (1.0 μM), Cu(OAc)₂ (1.0 μM), and 1.0–4.0 μM picolinate or alanine in PIPES buffer (10 mM, pH 6.1) at 25 °C. Experiments with the protein conjugate contained 5.0 μM ALBP-Phen-Cu(II) and 5.0–20 μM picolinate or alanine in PIPES buffer (10 mM, pH 6.1) at 25 °C. Fluorescence emission spectra from 300–450 nm were obtained by excitation at 275 nm (5.0 nm slits for both monochrometers, 100 nm/min scan speed). After titration, samples were incubated at 25 °C in the dark, spectra were recorded, and EDTA was added to a final concentration of 500 μM . A final spectrum was recorded after EDTA addition.

Electrospray Mass Spectrometry. Samples for mass spectrometry were obtained by extensive dialysis of solutions of ALBP and ALBP-Phen in 200 mM HEPES (1 mL, 1.1 mg/mL) against H₂O/MeOH/HOAc (89/10/1, v/v/v), (2 × 1 L). Spectra were obtained using a PE SCIEX API III MS/MS instrument, and the masses of ALBP and ALBP-Phen were determined by analysis of the intensity versus m/z data using HyperMass software.

Gel Filtration Chromatography. Gel filtration chromatography was performed using an FPLC system (Pharmacia) and a Superose 12 HR 10/30 column. Samples (100 μL) were eluted with 25 mM HEPES, pH 7.5, and 150 mM NaCl at a flow rate of 0.5 mL/min at 4 °C. The column was calibrated using bovine lung aprotinin (6500 g/mol), horse heart cytochrome *c* (12 400 g/mol), bovine erythrocyte carbonic anhydrase (29 000 g/mol), and bovine serum albumin (66 000 g/mol) as standards.

Protein Denaturation Experiments. The denaturation of ALBP and ALBP-Phen was followed spectrofluorometrically by monitoring the emission maximum upon excitation at 280 nm (5.5 nm excitation slitwidth, 7.5 nm emission slitwidth) in a cuvette thermostated to 25 °C. Samples contained ALBP or ALBP-Phen (1.0 μM), Tris·HCl (50 mM, pH 7.4), EDTA (0.1 mM), and guanidinium chloride (0–5.0 M). Data were fitted to a two state model, previously used for lipid binding proteins, described by Frieden and co-workers.³² To facilitate com-

parison between ALBP and ALBP-Phen, the data were scaled from 0 to 1 using the relationship $F_{\text{rel}} = (F - F_{\text{min}})/(F_{\text{max}} - F_{\text{min}})$ where F_{rel} is the relative fluorescence, and F_{max} and F_{min} are the maximum and minimum fluorescence values observed for the particular protein, respectively.

Amino Acid Ester Hydrolysis Reactions. Hydrolysis reactions contained racemic amino acid ester **6a**, **6b**, **6c**, **8a**, **8b**, or **10** (1 mM) and ALBP-Phen-Cu(II) (25 μM) in PIPES buffer (10 mM, pH 6.1) in a total reaction volume of 52 μL and were performed in microcentrifuge tubes at room temperature or in a thermostated water bath. At given time points, 5.0 μL aliquots of the reaction mixture were removed and quenched with 17 μL of H₂O and 3.0 μL of 100 mM EDTA and frozen at –20 °C until analysis.

Derivatization. Immediately before analysis, reaction samples were thawed, and 8.0 μL of the resulting material was derivatized with 8.0 μL of a reagent consisting of *N*-acetyl-L-cysteine dissolved in "Incomplete *o*-Phthaldialdehyde Reagent Solution" (Sigma no. P7914) at a concentration of 5 mg/mL; these reagents convert enantiomeric amines into diastereomeric isoindoles. The derivatization reaction was allowed to proceed for 5 min at which time the sample was immediately analyzed by HPLC.

HPLC Analysis. All reaction mixtures were separated by reversed phase HPLC using a Rainin Microsorb-MV C₁₈ column (5 μm , 4.6 × 250 mm). Chromatography was performed by injecting a 10 μL sample and eluting with a flow rate of 0.75 mL/min using a gradient of solvent A (80 mM sodium citrate and 20 mM sodium phosphate, pH 6.8, containing 10% MeOH) and solvent B (MeOH). Detection of the isoindole derivatives was achieved using a Beckman 6300A fluorescence detector (356 nm excitation filter and 450 nm emission filter), and integration was performed with a HP 3393A integrator or System Gold software. Response factors for the diastereomeric derivatives were obtained from calibration curves generated by derivatization and analysis of standard solutions of racemic amino acids. For alanine (**7**), an elution profile consisting of isocratic elution with 80% solvent A for 5 min followed by a 10 min linear gradient from 20% to 40% solvent B and further elution with 60% solvent A was employed. Using this system, the retention times for the D-alanine and L-alanine derivatives were 22.5 and 23.8 min, respectively. For tyrosine (**9**), an elution profile consisting of isocratic elution with 70% solvent A for 5 min followed by a 5 min linear gradient from 30% to 35% solvent B and further isocratic elution with 65% solvent A giving retention times for the L-tyrosine and D-tyrosine derivatives of 21.2 and 25.1 min, respectively. Serine (**11**) was separated using isocratic conditions (10% solvent B) with a flow rate of 0.65 mL/min. Under these conditions, the D-serine and L-serine derivatives eluted with retention times of 15.8 and 17.0 min, respectively.

PNPE (3) Hydrolysis. The rate of hydrolysis of picolinic acid *p*-nitrophenyl ester (**3**) was determined by measuring the increase in absorbance at 316 nm due to the formation of *p*-nitrophenol (**5**). The reactions contained ALBP-Phen-Cu(II) or CuSO₄ (10 μM) and PNPE (100 μM) in PIPES buffer (10 mM, pH 6.1) and were performed in quartz cuvettes at 25 °C. Absorbance values were converted to concentrations using a standard curve of *p*-nitrophenol (**5**) obtained in PIPES.

PMNA (12) Hydrolysis. The rate of hydrolysis of picolinic acid nitromethyl anilide **12** (PMNA) was determined by measuring the increase in absorbance at 400 nm due to the formation of *N*-methyl-4-nitroaniline (**13**). The reactions contained ALBP-Phen-Cu(II) (4.8 μM) and PMNA (20 μM –2 mM) in PIPES buffer (10 mM, pH 6.1) and were performed in microcentrifuge tubes in a 37 °C water bath. At various times the solutions were removed from the water bath and equilibrated to room temperature and the absorbances at 400 nm were measured. The rate of background hydrolysis of PMNA was determined from similar experiments performed in the absence of ALBP-Phen. Additional control experiments used ALBP or 4.8 μM CuSO₄. Absorbance values for *N*-methyl-4-nitroaniline in PIPES were converted to concentrations using a value of $\epsilon_{400} = 17\,600 \text{ M}^{-1}\text{cm}^{-1}$ calculated from a standard curve obtained in PIPES. All reactions were performed in duplicate and the data averaged.

(31) Riddles, P. W.; Blakeley, R. L.; Zerner, B. *Methods Enzymol.* **1983**, *91*, 49–59.

(32) Ropson, I. J.; Gordon, J. I.; Frieden, C. *Biochemistry* **1990**, *29*, 9591–9599.

Acknowledgment. The authors thank M. Silbergliitt and S. Flaim for modeling ALBP-Phen, C. Lambert for performing the denaturation experiments, L. Banaszak for providing the X-ray coordinates of ALBP, and D. Bernlohr for the plasmid pMON4. This work was supported by grants from the National Science Foundation (NSF-CHE-9506793) and the Petroleum Research Fund (PRF#28140-G4). R.R.D. was supported by a National Institutes of Health training grant (NIH 2T32GM08347-06).

Note Added in Proof. X-ray crystallographic analysis of the structure of ALBP-Phen indicates that the phenanthroline

ligand is sequestered within the protein cavity in a fashion similar to the model shown in Figure 1.²⁶

Supporting Information Available: Stereoviews of the ALBP-Phen model constructed with Insight Software and additional UV data for titrations of phenanthroline-Cu(II) with picolinate and alanine (5 pages). See any current masthead for ordering and Internet access instructions.

JA970820K